
Towards Optimal Compression: Joint Pruning and Quantization

Ben Zandonati
University of Cambridge
baz23@cam.ac.uk

Glenn Bucagu
University of Zürich
glennanta.bucagu@uzh.ch

Adrian Alan Pol
Princeton University
ap6964@princeton.edu

Maurizio Pierini
CERN
maurizio.pierini@cern.ch

Olya Sirkin, Tal Kopetz
CEVA, Inc
{olya.sirkin, tal.kopetz}@ceva-dsp.com

Abstract

Model compression is instrumental in optimizing deep neural network inference on resource-constrained hardware. The prevailing methods for network compression, namely quantization and pruning, have been shown to enhance efficiency at the cost of performance. Determining the most effective quantization and pruning strategies for individual layers and parameters remains a challenging problem, often requiring computationally expensive and ad hoc numerical optimization techniques. This paper introduces FITCompress, a novel method integrating layer-wise mixed-precision quantization and unstructured pruning using a unified heuristic approach. By leveraging the Fisher Information Metric and path planning through compression space, FITCompress optimally selects a combination of pruning mask and mixed-precision quantization configuration for a given pre-trained model and compression constraint. Experiments on computer vision and natural language processing benchmarks demonstrate that our proposed approach achieves a superior compression-performance trade-off compared to existing state-of-the-art methods. FITCompress stands out for its principled derivation, making it versatile across tasks and network architectures, and represents a step towards achieving optimal compression for neural networks.

1 Introduction

Deep neural networks (DNNs) require substantial computational resources for both training and deployment. However, many real-world applications involve devices with limited computational capabilities, such as mobile phones, embedded systems, or edge devices [1, 2, 3, 4]. Consequently, the demand for *model compression* [5] methods has surged with the scaling of large computer vision and natural language processing (NLP) foundational models. These methods are typically designed to reduce model size, latency, energy or memory consumption, while minimizing performance loss.

Pruning and *quantization* methods address these issues by reducing the memory footprint and computational requirements of neural networks while maintaining acceptable performance levels.

Quantization reduces the precision of network parameters, typically from floating-point to fixed-point representation. By using fewer bits to represent each parameter, quantization significantly reduces the memory requirements and computational complexity of network operations. This is especially beneficial for hardware platforms that have limited memory and processing power such as FPGAs. Quantization can be performed homogeneously (i.e., using the same bit-width for the whole network), but empirical evidence suggests that each layer in a model exhibits a different sensitivity to

quantization [6]. This calls for *mixed-precision quantization* (MPQ) [7]. The challenge, in this case, is the combinatorial explosion in the search space of possible MPQ configurations as networks grow. In particular, the time complexity is in $\mathcal{O}(|B|^{2L})$, where B is the set of considered bit-widths and L is the number of layers.

Pruning selectively removes unnecessary connections or parameters from the network, effectively reducing its size. It exploits the observation that many network parameters are redundant or contribute minimally to overall network performance. As with MPQ, as networks grow, the number of possible pruning masks to apply grows exponentially in $\mathcal{O}(2^{|\Theta|})$, where $|\Theta|$ is the number of parameters in the network. Previous works typically employ heuristic-based methods to determine parameter importance and prune accordingly. By removing such parameters, pruning reduces the model size, memory footprint, and computational requirements during inference.

Recent attempts have been made to optimally quantize and prune networks to improve the performance-compression trade-off for significant compression levels. Such methods typically employ slow, ad hoc, black-box or first-order optimization methods, the results of which are not guaranteed to generalize to future foundational models and challenging architectures. In particular, many methods sequentially prune then quantize [8], and do not consider the two under the same theoretical framework.

In this work, we introduce FITCompress, a principled algorithm that combines MPQ and pruning for one-shot optimal network compression. By modelling MPQ and pruning under the Fisher Information Metric (FIM), we provide a method to integrate these two compression techniques. In doing so, we leverage modern platforms that support sparse and quantized formats [9, 10, 11]. This framework enables us to measure distances in the parameter space associated with compression. Moreover, we introduce a reduced action space for quantization and pruning, referred to as the *compression space*. By traversing this space using simple path-planning techniques, we obtain compression configurations that satisfy the required resource constraints while minimizing the performance drop of a pre-trained model. FITCompress approximates perturbations in the parameter space and takes iterative steps towards achieving optimal compression.

Our main contributions are summarized as follows:

1. This paper introduces FITCompress, a principled algorithm that combines quantization and pruning under FIM to improve network compression. FITCompress provides a method to integrate these techniques, measures distances in the parameter space associated with compression, and traverses a reduced action space to find optimal compression configurations in one-shot.
2. Empirically, we show state-of-the-art compression ratios across a diverse set of architectures and datasets. The architectures evaluated include LeNet-5, VGG-7, ResNet-18, ResNet-34, ResNet-50, BERT-Base, and YOLOv5. The datasets include MNIST, CIFAR-10, ImageNet, SST-2, MNLI-m, SQuAD and COCO. Via this extensive evaluation, we highlight the strong performance and generality of FITCompress.

2 Related Work

FITCompress employs layer-wise mixed-precision quantization and unstructured pruning. That is, quantization is performed at the granularity of layers, while pruning is performed at the granularity of individual parameters. Both are well supported in modern deep learning frameworks. Additionally, after quantization and pruning, further training is performed to recover lost performance. Such quantization-aware training (QAT) [12] is commonly employed by machine learning practitioners, and by all of our evaluation benchmarks (except where specified for YOLOv5 [13]). To that end, we present a brief taxonomy of relevant MPQ and pruning methods. For more comprehensive summaries of related work, we refer readers to the appropriate reviews [14, 15, 16].

Pruning. Unstructured pruning involves removing individual model parameters according to a simple-to-compute heuristic. This can include the magnitude [17, 8, 18], first-order information [19, 20, 21, 22, 23, 24, 25], or second-order information [26, 27, 28]. These methods suffer from *layer collapse*, in which all (or a significant number) of the weights in a single layer are pruned, rendering training and inference impossible. This issue is alleviated by conserving what [29] refer to as synaptic saliency. While iterative pruning methods help to conserve synaptic saliency, better

metrics (such as the Fisher Information [30, 31]) further boost pruning performance. Our work employs an approximation of FIM, iteratively computed as we move through the compression space.

Mixed-Precision Quantization. Second-order information is commonly used to effectively quantize neural networks. For example, in computer vision, [32, 6, 33] used the Hessian’s top eigenvalues/trace to determine a layer’s sensitivity to the perturbations associated with a reduction in bit precision. For NLP tasks, [34] defined sensitivity measurement based on both the mean and variance of the top Hessian eigenvalues to generate MPQ configurations. Other black-box approaches have been proposed, including multi-stage optimization [35, 36], linear programming [37, 38], deep reinforcement learning (DRL) [39, 40, 41], and neural architecture search (NAS) [42, 7] however these methods are computationally expensive. Recently, the Fisher Information Trace (FIT) [43] emerged as the superior metric for model sensitivity to quantization, being computationally inexpensive and correlating highly with final model performance. This work uses an extension of FIT, to cope with the significant deviations in the parameter space.

Joint Pruning and Quantization. Combining pruning and quantization is nontrivial. Bayesian and variational approaches are commonly used [44, 45, 46, 47] but are difficult to scale to larger models. Hessian-based methods have been proposed [48], but suffer from slow computation. More recently, [49] used non-linear constrained optimisation to analytically solve the joint MPQ and pruning problem. Notably, the method requires two fine-tuning stages. Similar multi-stage frameworks that prune then quantize were also introduced by [8] and [50]. However, [51] empirically demonstrated the non-commutativity of pruning and quantization across generative and discriminatory tasks. This is one of the primary motivations for the path-planning approach in FITCompress. In summary, FITCompress differentiates itself by unifying and interleaving quantization and pruning under the computationally inexpensive Fisher Information.

3 Methodology

Consider a dataset $D = \{(x, y)_i\}_1^N$ drawn i.i.d. from the true underlying joint distribution of samples. With this dataset, a parameterized model is trained to estimate the conditional distribution $p(y|x, \theta) = p_\theta$, where the parameters $\theta \in \Theta$ are chosen to minimize the loss function $\mathcal{L}_\theta(x, y) : \mathcal{X} \times \mathcal{Y} \rightarrow \mathbb{R}$ via gradient descent. The parameterized model p_θ is a DNN consisting of L layers.

In this paper, we consider both layer-wise MPQ and unstructured pruning. Consequently, compression involves choosing each layer’s bit-width $\{Q_i\}_1^L$ and providing a pruning mask $P \in \{0, 1\}^{|\Theta|}$. We will describe pruning in terms of the induced compression $\kappa = \frac{\sum P}{|\Theta|}$, where $\sum P$ is the number of masked parameters, and $|\Theta|$ is the total number of parameters in the model. Each layer-wise quantization and pruning mask defines a configuration $c \in \mathcal{C}^{L+|\Theta|}$ in the *compression space*.

As noted in Section 2, searching this space, such that model performance is retained after compression, is the subject of ongoing research. In particular, principled methods derived from the Fisher Information [31, 43] yield high-performing models at low compression rates.

3.1 FIT: Metric for Parameter Sensitivity

Consider a general perturbation to the model parameters: $p_{\theta+\delta\theta}$, which could arise as a result of quantization or pruning. To measure the effect of this perturbation on the model, we use the KL divergence:

$$D_{KL}(p_\theta || p_{\theta+\delta\theta}) = \frac{1}{2} \delta\theta^T I(\theta) \delta\theta$$

Where the FIM [52], $I(\theta)$, takes the following form (for a typical cross-entropy loss function):

$$I(\theta) = \mathbb{E}(\nabla_\theta \log p_\theta \nabla_\theta \log p_\theta^T) \tag{1}$$

As noted in Section 2, recent work [43] numerically approximates this distance in the parameter space associated with quantization. The resulting FIT metric proved an effective, and computationally inexpensive, quantization heuristic (shown here in empirical form):

$$FIT(\theta, \delta\theta) = \sum_l^L \frac{1}{n(l)} \cdot Tr(\hat{I}(\theta_l)) \cdot \|\delta\theta\|_l^2 \tag{2}$$

Where $n(l)$ denotes the specific number of parameters in a single layer l , and $Tr(\hat{I}(\theta_l))$ denotes the trace of the empirical Fisher \hat{I} for the set of parameters θ_l in a single layer l .

From an information geometric perspective, it is well known [52, 53] that this formulation relies on a first-order divergence approximation, valid for small perturbations. It is clear that at very low bit precision and high pruning rates (that is to say, significant compression), this approximation is broken. More precisely, we move too far from the original model in the tangent space of our statistical manifold (induced by p_θ). For a more detailed derivation, see Appendix A.

3.2 Pruning with FIT

The consequences of beyond-small approximations have been indirectly addressed by the pruning literature. Recent work [20] highlights the importance of the pruning criterion itself and [29] shows that iterative pruning methods improve upon single-shot schemes.

From a geometric perspective, standard magnitude pruning assumes that the local metric tensor is an identity function. Similarly, non-iterative methods assume that the local tangent space is sufficiently representative of the statistical manifold, such that the metric remains constant. As shown in Figure 1, removing both assumptions in the example of LeNet-5 on CIFAR-10 improves empirical performance. This repeats the findings of [29].

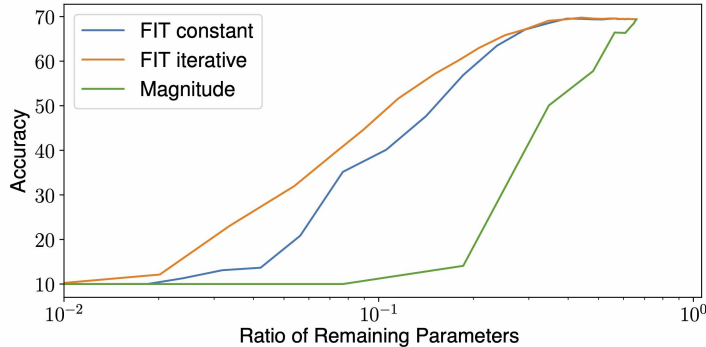


Figure 1: Fraction of non-zero parameters, κ , and accuracy after each iteration of pruning LeNet-5 on CIFAR-10 dataset. The lower the κ , the higher the compression ratio.

3.3 Scheduling through Path Planning

Equipping algorithms with a distance to explore compression space effectively is of central importance. When moving beyond local perturbations, the Fisher-Rao distance is obtained [54]:

$$g = \int [\delta\theta^T I(\theta)\delta\theta]^{\frac{1}{2}} \quad (3)$$

From this perspective, we define *optimal compression*.

Definition 3.1. (Optimal Compression) An optimal compression configuration c^* for a given constraint α is the solution to the following:

$$c^* = \arg \min_c \left(\int_{S(\theta, \theta_c)} [\delta\theta^T I(\theta)\delta\theta]^{\frac{1}{2}} \right) \quad (4)$$

Where $S(\theta, \theta_c)$ refers to the geodesic (shortest) path, and θ_c obeys the compression constraint, i.e. $\alpha_c \leq \alpha$.

Direct use of Definition 3.1 is not possible. Compression space is discrete, and the evaluation of this integral is not computationally feasible. Both the final compression configuration, as well as the shortest path $S(\theta, \theta_c)$ are unknown. Instead, we look to approximations of Definition 3.1.

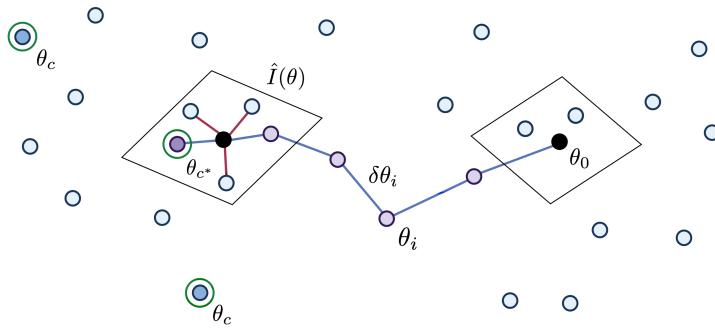


Figure 3: Illustration of the FITCompress algorithm, path planning through compression space. θ_0 is the starting parameter set. θ_c denotes hypothetical configuration and θ_{c^*} is the optimal one. Using a single contribution to \hat{g} for complete compression can become a false compass, as the optimal intermediate steps are not considered. Compressing the model directly could lead the algorithm to θ_c instead of θ_{c^*} . Thus, inclusion of path planning is one of our central contributions.

Algorithm 1 FITCompress: Single-Shot Compression

Require: Pre-trained model p_{θ_0} , training dataset D , Quantization Schedule Q , Pruning Schedule κ , Desired Compression Constraint α .

Input: initial parameters θ_0 , distance $\hat{g}_0 = 0$, initial configuration $c_i = [32, 32, \dots, 32, 0]$
 $i = 0$

repeat
 candidate distance = ∞
 for $j = 0$ **to** $L + 1$ **do**
 Candidate configuration: $c_j = c_i + a_j$
 Candidate parameters: $\theta_j = \theta_{i,c_j}$
 Candidate compression rate: α_j
 $\hat{g}_j = \hat{g}_i + FIT(\theta_i, \delta\theta_{i,j})^{\frac{1}{2}}$
 $\hat{f}_j = |\alpha_j - \alpha| FIT(\theta_j, \theta_j)^{\frac{1}{2}}$
 if $\hat{g}_j + \lambda \hat{f}_j <$ candidate distance **then**
 $\theta_{i+1} = \theta_j$
 $\hat{g}_{i+1} = \hat{g}_j$
 candidate distance = $\hat{g}_j + \lambda \hat{f}_j$
 end if
 end for
 $i = i + 1$
until $\alpha_i \leq \alpha$

4 Experiments

In the section, we apply FITCompress in a wide range of computer vision and NLP tasks. We compare FITCompress to the current state-of-the-art methods that provide their quantization configurations and pruning masks, which allows us to compute the compression metric.

4.1 Compression Metric

There are many possible target devices for neural network deployment, each with their own idiosyncrasies, storage, processing methods, and costs. Efficiency greatly depends on specific kernel-implementations, and inference latency or power consumption might be a deceptive indicator of compression. FITCompress is designed to be hardware-agnostic. We therefore use the percentage of Bit-Operations (BOPs) relative to the full-precision unpruned model as a proxy metric for compression. The BOPs metric generalizes floating-point operations (FLOPs) and multiply-and-accumulate

operations (MACs) to heterogeneously quantized neural networks because they cannot be efficiently used to evaluate integer arithmetic operations [56]. This metric is commonly used in the network compression literature, and we follow its implementation from [57] and [46].

4.2 Experiments on Low Resolution Image Classification

In the first set of experiments, we use LeNet-5 (4.37 GBOPs) and VGG-7 (631 GBOPs) to evaluate FITCompress on MNIST [58] and CIFAR-10 [59], respectively. In each experiment, we report the mean top-1 accuracy change over 3 runs. The experiment results are reported in Table 1. Experiment details are provided in Table 4 from Appendix C. We compare FITCompress to pruning-only methods (GAL [60], AFP [61], CFP [62], and HBFP [63]), an MPQ-only method (DQ [64]), and joint pruning-MPQ methods (DJPQ [47] and BB [46]). We only consider recently published methods that provide model pruning masks and quantization configurations as these are required to compute BOPs.

We observe that FITCompress compresses LeNet-5 to 78% of the rate reported by BB, while losing half the accuracy lost by the BB-generated model. Similarly, FITCompress compresses VGG-7 to 79% and 48% of the rates reported by BB and DJPQ respectively, while gaining 0.02% accuracy. In contrast, the BB and DJPQ models lose 1.09% and 1.51% accuracy respectively. BB performs aggressive quantization (most LeNet-5 and VGG-7 layers in 2 bits) with very light pruning. DJPQ performs moderate quantization (most VGG-7 layers in 4 bits) with aggressive pruning in the first 3 layers. In contrast, FITCompress provides moderate quantization (LeNet-5 layers in 3-4 bits and VGG-7 layers in 3-5 bits) with 97.6% and 94.1% pruning on LeNet-5 and VGG-7 respectively. FITCompress configurations are in Appendix D. FITCompress provides a practical advantage over methods that only consider structured pruning (e.g., DJPQ and BB). See Appendix E for details.

Table 1: Results for LeNet-5 on MNIST and VGG-7 on CIFAR-10. "-" indicates that the corresponding results are not reported in the literature. We define *precision* as W/A, where W and A are the bit-widths assigned to weights and activations respectively. "M" indicates heterogeneous bit-width. We include our own full-precision (FP) baseline model performance. "†" indicates an MPQ setting restricted to power-of-two bit-widths.

Method	Precision	LeNet-5 on MNIST (FP Acc: 99.36%)		VGG-7 on CIFAR-10 (FP Acc: 93.05%)	
		Δ Acc. (%)	Rel. BOPs (%)	Δ Acc. (%)	Rel. BOPs (%)
GAL	32/32	-0.21	4.40	-	-
AFP	32/32	-1.47	3.59	-	-
CFP	32/32	-0.86	2.02	-	-
HBFP	32/32	-0.57	2.02	-	-
DQ [†]	M/M	-	-	-1.46	0.54
DQ	M/M	-	-	-1.46	0.48
DJPQ	M/M	-	-	-1.51	0.48
DJPQ [†]	M/M	-	-	-1.62	0.46
BB	M/M	-0.06 \pm 0.03	0.36 \pm 0.01	-1.09 \pm 0.04	0.29 \pm 0.00
FITCompress	M/M	-0.03 \pm 0.00	0.28 \pm 0.01	+0.02 \pm 0.06	0.23 \pm 0.01
FITCompress[†]	M/M	-0.10 \pm 0.06	0.44 \pm 0.00	-1.03 \pm 0.02	0.29 \pm 0.01

4.3 Experiments on Higher Resolution Image Classification

In the second set of experiments, we use ResNet-18 (1858 GBOPs), ResNet-34 (3752 GBOPs), and ResNet-50 (4187 GBOPs) and evaluate FITCompress on ImageNet [65]. We report the mean top-1 accuracy change over 3 runs. Experiment details are provided in Table 4 from Appendix C. We compare FITCompress to pruning-only methods (Taylor [21], LCCL [66], SOKS [67], ASKs [68], BC-Net [69], PFP-B [70], CCEP [71] and HBFP [63]), MPQ-only methods (DNAS [7], HAWQ-V3 [33] and HAQ [41]), and joint pruning-MPQ methods (VIBNet+DQ [72, 64], OBC [48], DJPQ [47] and BB [46]). The results are shown in Table 2. We observe that FITCompress provides the best model size vs. performance trade-off even on a complex dataset like ImageNet on larger networks like variations of ResNet. Unlike BB and DJPQ, which perform aggressive quantization and light pruning, FITCompress provides more balance between pruning and quantization. FITCompress configurations are shown in Appendix D. In Figure 4, we illustrate how FITCompress interleaves pruning and quantization to compress ResNet-18 on ImageNet.

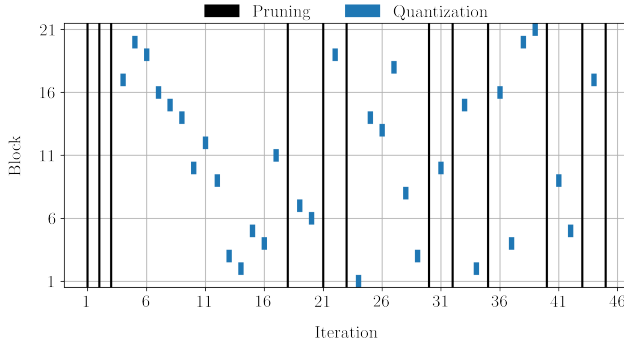


Figure 4: An example of FITCompress’ compression path using ResNet-18 on ImageNet. At each iteration, FITCompress chooses whether a given layer (indexed on the vertical axis from 1-21) should be quantized or pruned (and if so by how much), until the desired model size is achieved.

Table 2: Results for ResNet-18, ResNet-34, and ResNet-50 on ImageNet. We report the mean performance change over 3 runs. "-" indicates that the corresponding results are not reported in the literature. We define *precision* as W/A, where W and A are the bit-widths assigned to weights and activations respectively. "M" indicates MPQ. We use the pre-trained models provided by PyTorch [73] and include the full-precision (FP) baseline model performance.

Method	Precision	ResNet-18 (FP Acc: 69.76%)		ResNet-34 (FP Acc: 73.31%)		ResNet-50 (FP Acc: 76.13%)	
		Δ Acc. (%)	Rel. BOPs (%)	Δ Acc. (%)	Rel. BOPs (%)	Δ Acc. (%)	Rel. BOPs (%)
Taylor	32/32	-	-	-0.48	75.20	-	-
LCCL	32/32	-3.65	65.40	-0.43	74.14	-	-
ASKs	32/32	-0.87	59.34	-0.47	57.34	-	-
PFP-B	32/32	-4.09	56.88	-	-	-	-
SOKS	32/32	-1.26	45.05	-0.49	44.02	-	-
BCNet	32/32	-	-	-	-	-0.46	48.90
CCEP	32/32	-	-	-	-	-1.26	35.91
HBFP	32/32	-	-	-	-	-5.69	25.55
HAQ	M/M	-	-	-	-	-0.67	13.20
OBC	M/M	-4.25	6.67	-3.01	6.67	-4.66	6.67
DNAS	M/M	-1.45	4.73	-0.75	5.26	-	-
HAWQ-V3	M/M	-2.75	2.91	-	-	-3.27	2.78
VIBNet+DQ	M/M	-1.22	2.13	-	-	-	-
DQ	M/M	-1.34	2.10	-	-	-	-
DJPQ	M/M	-0.94	1.67	-	-	-	-
BB	M/M	-1.51 \pm 0.18	1.38 \pm 0.03	-	-	-	-
FITCompress	M/M	-0.92 \pm 0.12	1.38 \pm 0.06	-0.95 \pm 0.15	2.80 \pm 0.08	-1.05 \pm 0.23	2.63 \pm 0.05

4.4 Experiments on NLP Tasks

Training a large, over-parameterized transformer and then compressing it results in better accuracy than training a smaller model directly [74]. In the third set of experiments, we apply FITCompress to BERT-Base [75] and evaluate model performance on SST-2 [76] and MNLI-m[77] from the GLUE benchmark [78], as well as SQuAD [79]. We compare FITCompress to a pruning-only method (FPTQFT [80]), a MPQ-only method (Q-BERT [34]), and a joint pruning-MPQ method (OBC [48]). For strong results, our training protocol includes knowledge distillation. Similarly to [34], activations and embeddings are kept at 8-bits. Experiment details are provided in Table 4 from Appendix C. The results are displayed in Table 3. We observe that FITCompress provides the best model size vs. performance trade-off. Notably, our results on NLP tasks suggest that BERT is challenging to compress, even with the combination of pruning and quantization. Complementary methods, such as the ones proposed in [81] could further speed up implementations and lower memory requirements.

4.5 Experiments on Object Detection

In the final set of experiments, we use the YOLOv5m [13] architecture on COCO [82] to evaluate FITCompress in an object detection task. We compare FITCompress to OBC [48]. To the best of our knowledge, no other works consider this learning task and architecture in a pruning or MPQ setting.

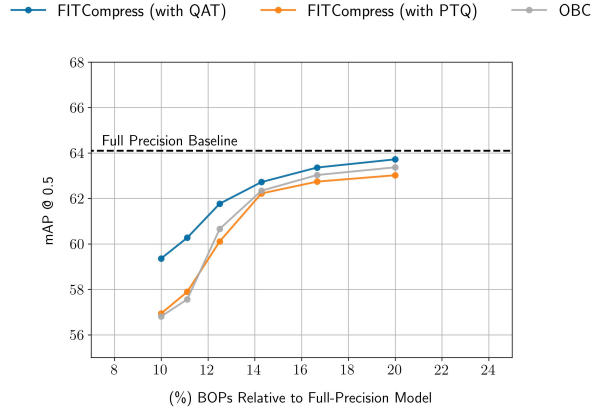


Figure 5: Comparing FITCompress and OBC across different compression constraints using YOLOv5m on COCO. We report the mean mAP at a threshold IoU of 0.5 over 3 runs.

Table 3: Results for BERT on various NLP tasks. We report the mean performance change over 3 runs.

	Method	Δ Performance	Rel. BOPs (%)
<i>SQuAD</i> (FP F_1 : 88.20)	FPTQFT	-1.76	60.00
	OBC	-4.71	10.00
	Q-BERT	-0.33	3.13
	FITCompress	0.33 ± 0.04	3.10 ± 0.04
<i>SST-2</i> (FP Acc: 92.66%)	FPTQFT	-1.08	60.00
	Q-BERT	-0.34	3.13
	FITCompress	-0.32 ± 0.06	3.10 ± 0.03
<i>MNLI-m</i> (FP Acc: 85.01%)	FPTQFT	-2.02	60.00
	Q-BERT	-0.11	3.13
	FITCompress	-0.13 ± 0.07	3.10 ± 0.04

For fair comparison, we extend FITCompress to a post-training quantization (PTQ) setting, that is, no QAT is performed. Experiment details are provided in Table 4 from Appendix C. Results are shown in Figure 5. FITCompress (with PTQ) yields better performance than OBC under 12% relative BOPs. In contrast, FITCompress with QAT yields superior performance for all compression constraints.

5 Conclusion

In this work, we presented FITCompress, a novel algorithm that leverages the FIM and employs path planning through compression space to effectively select a combination of pruning mask and MPQ configuration. Our experimental evaluations on various computer vision and natural language processing benchmarks demonstrate that FITCompress outperforms existing state-of-the-art methods, achieving a superior compression-performance trade-off.

Broader Impact and Future Work. FITCompress is a general model compression algorithm that can facilitate the training and deployment of efficient neural networks. On one hand, this could increase the efficiency of models deployed on edge devices (e.g. less power consumption for models deployed on servers, and longer battery lives for models running on mobile devices). Our work could be viewed in the context of democratizing machine learning and providing access to those without industrial-scale compute. On the other hand, compression might have unpredictable effects on a given model. [83] suggests that sparse models may affect individual classes instead of aggregate statistics, potentially yielding unfair models. We encourage further research in this direction for compressed and fair models. For even stronger results, one could combine FITCompress with state-of-the-art quantization implementations such as LSQ [84] and PACT [85].

References

- [1] Claudionor N. Coelho, Aki Kuusela, Shan Li, Hao Zhuang, Jennifer Ngadiuba, Thea Klæboe Aarrestad, Vladimir Loncar, Maurizio Pierini, Adrian Alan Pol, and Sioni Summers. Automatic heterogeneous quantization of deep neural networks for low-latency inference on the edge for particle detectors. *Nature Machine Intelligence*, 3(8):675–686, jun 2021.
- [2] Xiangzhong Luo, Di Liu, Hao Kong, and Weichen Liu. Edgenas: Discovering efficient neural architectures for edge systems. In *2020 IEEE 38th International Conference on Computer Design (ICCD)*, pages 288–295, 2020.
- [3] Zhaolong Ning, Peiran Dong, Xiaojie Wang, Xiping Hu, Lei Guo, Bin Hu, Yi Guo, Tie Qiu, and Ricky Y. K. Kwok. Mobile edge computing enabled 5g health monitoring for internet of medical things: A decentralized game theoretic approach. *IEEE Journal on Selected Areas in Communications*, 39(2):463–478, 2021.
- [4] Mi Zhang, Faen Zhang, Nicholas D. Lane, Yuanchao Shu, Xiao Zeng, Biyi Fang, Shen Yan, and Hui Xu. Deep learning in the era of edge computing: Challenges and opportunities, 2020.
- [5] Vivienne Sze, Yu-Hsin Chen, Tien-Ju Yang, and Joel S Emer. Efficient processing of deep neural networks: A tutorial and survey. *Proceedings of the IEEE*, 105(12):2295–2329, 2017.
- [6] Zhen Dong, Zhewei Yao, Amir Gholami, Michael W Mahoney, and Kurt Keutzer. Hawq: Hessian aware quantization of neural networks with mixed-precision. In *Proceedings of the IEEE/CVF International Conference on Computer Vision*, pages 293–302, 2019.
- [7] Bichen Wu, Yanghan Wang, Peizhao Zhang, Yuandong Tian, Peter Vajda, and Kurt Keutzer. Mixed precision quantization of convnets via differentiable neural architecture search. *arXiv preprint arXiv:1812.00090*, 2018.
- [8] Song Han, Huizi Mao, and William J. Dally. Deep compression: Compressing deep neural networks with pruning, trained quantization and Huffman coding, 2016.
- [9] Eugenia Iofinova, Alexandra Peste, Mark Kurtz, and Dan Alistarh. How well do sparse imagenet models transfer? *CoRR*, abs/2111.13445, 2021.
- [10] Mark Kurtz, Justin Kopinsky, Rati Gelashvili, Alexander Matveev, John Carr, Michael Goin, William Leiserson, Sage Moore, Bill Nell, Nir Shavit, and Dan Alistarh. Inducing and exploiting activation sparsity for fast inference on deep neural networks. In Hal Daumé III and Aarti Singh, editors, *Proceedings of the 37th International Conference on Machine Learning*, volume 119 of *Proceedings of Machine Learning Research*, pages 5533–5543, Virtual, 13–18 Jul 2020. PMLR.
- [11] Asit Mishra, Jorge Albericio Latorre, Jeff Pool, Darko Stosic, Dusan Stosic, Ganesh Venkatesh, Chong Yu, and Paulius Micikevicius. Accelerating sparse deep neural networks, 2021.
- [12] Benoit Jacob, Skirmantas Kligys, Bo Chen, Menglong Zhu, Matthew Tang, Andrew Howard, Hartwig Adam, and Dmitry Kalenichenko. Quantization and training of neural networks for efficient integer-arithmetic-only inference. In *Proceedings of the IEEE conference on computer vision and pattern recognition*, pages 2704–2713, 2018.
- [13] Glenn Jocher, Ayush Chaurasia, Alex Stoken, Jirka Borovec, NanoCode012, Yonghye Kwon, Kalen Michael, TaoXie, Jiacong Fang, Imyhxy, , Lorna, Zeng Yifu, Colin Wong, Abhiram V, Diego Montes, Zhiqiang Wang, Cristi Fati, Jébastin Nadar, Laughing, UnglvKitDe, Victor Sonck, Tkianai, YxNONG, Piotr Skalski, Adam Hogan, Dhruv Nair, Max Strobel, and Mrinal Jain. ultralytics/yolov5: v7.0 - yolov5 sota realtime instance segmentation, 2022.
- [14] Davis Blalock, Jose Javier Gonzalez Ortiz, Jonathan Frankle, and John Guttag. What is the state of neural network pruning? *Proceedings of machine learning and systems*, 2:129–146, 2020.
- [15] Torsten Hoeftler, Dan Alistarh, Tal Ben-Nun, Nikoli Dryden, and Alexandra Peste. Sparsity in deep learning: Pruning and growth for efficient inference and training in neural networks. *J. Mach. Learn. Res.*, 22(241):1–124, 2021.

- [16] Markus Nagel, Marios Fournarakis, Rana Ali Amjad, Yelysei Bondarenko, Mart van Baalen, and Tijmen Blankevoort. A white paper on neural network quantization. *arXiv preprint arXiv:2106.08295*, 2021.
- [17] Trevor Gale, Erich Elsen, and Sara Hooker. The state of sparsity in deep neural networks, 2019.
- [18] Steven A. Janowsky. Pruning versus clipping in neural networks. *Physical Review A*, 39(12):6600–6603, 1989.
- [19] Jaeho Lee, Sejun Park, Sangwoo Mo, Sungsoo Ahn, and Jinwoo Shin. Layer-adaptive sparsity for the magnitude-based pruning, 2021.
- [20] Namhoon Lee, Thalaiyasingam Ajanthan, and Philip HS Torr. Snip: Single-shot network pruning based on connection sensitivity. *arXiv preprint arXiv:1810.02340*, 2018.
- [21] Pavlo Molchanov, Arun Mallya, Stephen Tyree, Iuri Frosio, and Jan Kautz. Importance estimation for neural network pruning. In *Proceedings of the IEEE/CVF Conference on Computer Vision and Pattern Recognition*, pages 11264–11272, 2019.
- [22] Michael C Mozer and Paul Smolensky. Skeletonization: A technique for trimming the fat from a network via relevance assessment. *Advances in neural information processing systems*, 1, 1988.
- [23] Victor Sanh, Thomas Wolf, and Alexander Rush. Movement pruning: Adaptive sparsity by fine-tuning. *Advances in Neural Information Processing Systems*, 33:20378–20389, 2020.
- [24] Chaoqi Wang, Guodong Zhang, and Roger Grosse. Picking winning tickets before training by preserving gradient flow. *arXiv preprint arXiv:2002.07376*, 2020.
- [25] Qingru Zhang, Simiao Zuo, Chen Liang, Alexander Bukharin, Pengcheng He, Weizhu Chen, and Tuo Zhao. Platon: Pruning large transformer models with upper confidence bound of weight importance, 2022.
- [26] Elias Frantar, Eldar Kurtic, and Dan Alistarh. M-fac: Efficient matrix-free approximations of second-order information, 2021.
- [27] Babak Hassibi and David Stork. Second order derivatives for network pruning: Optimal brain surgeon. *Advances in neural information processing systems*, 5, 1992.
- [28] Yann LeCun, John Denker, and Sara Solla. Optimal brain damage. *Advances in neural information processing systems*, 2, 1989.
- [29] Hidenori Tanaka, Daniel Kunin, Daniel L Yamins, and Surya Ganguli. Pruning neural networks without any data by iteratively conserving synaptic flow. *Advances in Neural Information Processing Systems*, 33:6377–6389, 2020.
- [30] Sidak Pal Singh and Dan Alistarh. Woodfisher: Efficient second-order approximation for neural network compression, 2020.
- [31] Lucas Theis, Iryna Korshunova, Alykhan Tejani, and Ferenc Huszár. Faster gaze prediction with dense networks and fisher pruning. *arXiv preprint arXiv:1801.05787*, 2018.
- [32] Zhen Dong, Zhewei Yao, Daiyaan Arfeen, Amir Gholami, Michael W Mahoney, and Kurt Keutzer. Hawq-v2: Hessian aware trace-weighted quantization of neural networks. *Advances in neural information processing systems*, 33:18518–18529, 2020.
- [33] Zhewei Yao, Zhen Dong, Zhangcheng Zheng, Amir Gholami, Jiali Yu, Eric Tan, Leyuan Wang, Qijing Huang, Yida Wang, Michael Mahoney, et al. Hawq-v3: Dyadic neural network quantization. In *International Conference on Machine Learning*, pages 11875–11886. PMLR, 2021.
- [34] Sheng Shen, Zhen Dong, Jiayu Ye, Linjian Ma, Zhewei Yao, Amir Gholami, Michael W Mahoney, and Kurt Keutzer. Q-bert: Hessian based ultra low precision quantization of bert. In *Proceedings of the AAAI Conference on Artificial Intelligence*, volume 34, pages 8815–8821, 2020.

- [35] Nilesh Prasad Pandey, Markus Nagel, Mart van Baalen, Yin Huang, Chirag Patel, and Tijmen Blankevoort. A practical mixed precision algorithm for post-training quantization, 2023.
- [36] Clemens JS Schaefer, Elfie Guo, Caitlin Stanton, Xiaofan Zhang, Tom Jablin, Navid Lambert-Shirzad, Jian Li, Chiachen Chou, Siddharth Joshi, and Yu Emma Wang. Mixed precision post training quantization of neural networks with sensitivity guided search, 2023.
- [37] Yuexiao Ma, Taisong Jin, Xiawu Zheng, Yan Wang, Huixia Li, Yongjian Wu, Guannan Jiang, Wei Zhang, and Rongrong Ji. Ompq: Orthogonal mixed precision quantization, 2022.
- [38] Chen Tang, Kai Ouyang, Zhi Wang, Yifei Zhu, Yaowei Wang, Wen Ji, and Wenwu Zhu. Mixed-precision neural network quantization via learned layer-wise importance, 2023.
- [39] Ahmed T. Elthakeb, Prannoy Pilligundla, FatemehSadat Mireshghallah, Amir Yazdanbakhsh, and Hadi Esmaeilzadeh. Releq: A reinforcement learning approach for deep quantization of neural networks, 2020.
- [40] Xu Qian, Victor Li, and Crews Darren. Channel-wise hessian aware trace-weighted quantization of neural networks, 2020.
- [41] Kuan Wang, Zhijian Liu, Yujun Lin, Ji Lin, and Song Han. Haq: Hardware-aware automated quantization with mixed precision. In *Proceedings of the IEEE/CVF Conference on Computer Vision and Pattern Recognition*, pages 8612–8620, 2019.
- [42] Zichao Guo, Xiangyu Zhang, Haoyuan Mu, Wen Heng, Zechun Liu, Yichen Wei, and Jian Sun. Single path one-shot neural architecture search with uniform sampling, 2020.
- [43] Ben Zandonati, Adrian Alan Pol, Maurizio Pierini, Olya Sirkin, and Tal Kopetz. Fit: A metric for model sensitivity. *arXiv preprint arXiv:2210.08502*, 2022.
- [44] Christos Louizos, Karen Ullrich, and Max Welling. Bayesian compression for deep learning, 2017.
- [45] Frederick Tung and Greg Mori. Clip-q: Deep network compression learning by in-parallel pruning-quantization. *2018 IEEE/CVF Conference on Computer Vision and Pattern Recognition*, 2018.
- [46] Mart Van Baalen, Christos Louizos, Markus Nagel, Rana Ali Amjad, Ying Wang, Tijmen Blankevoort, and Max Welling. Bayesian bits: Unifying quantization and pruning. *Advances in neural information processing systems*, 33:5741–5752, 2020.
- [47] Ying Wang, Yadong Lu, and Tijmen Blankevoort. Differentiable joint pruning and quantization for hardware efficiency. In *European Conference on Computer Vision*, pages 259–277. Springer, 2020.
- [48] Elias Frantar and Dan Alistarh. Optimal brain compression: A framework for accurate post-training quantization and pruning. In Alice H. Oh, Alekh Agarwal, Danielle Belgrave, and Kyunghyun Cho, editors, *Advances in Neural Information Processing Systems*, 2022.
- [49] Peng Hu, Xi Peng, Hongyuan Zhu, Mohamed M. Sabry Aly, and Jie Lin. Opq: Compressing deep neural networks with one-shot pruning-quantization, 2022.
- [50] Po-Hsiang Yu, Sih-Sian Wu, Jan P. Klopp, Liang-Gee Chen, and Shao-Yi Chien. Joint pruning & quantization for extremely sparse neural networks, 2020.
- [51] Xinyu Zhang, Ian Colbert, Ken Kreutz-Delgado, and Srinjoy Das. Training deep neural networks with joint quantization and pruning of weights and activations, 2021.
- [52] Shun-ichi Amari. *Information geometry and its applications*, volume 194. Springer, 2016.
- [53] Frank Nielsen. An elementary introduction to information geometry. *Entropy*, 22(10):1100, 2020.
- [54] Colin Atkinson and Ann FS Mitchell. Rao’s distance measure. *Sankhyā: The Indian Journal of Statistics, Series A*, pages 345–365, 1981.

- [55] Stuart Russell and Peter Norvig. *Artificial Intelligence: A Modern Approach (4th Edition)*. Pearson, 2020.
- [56] Pedro J. Freire, Sasipim Srivallapanondh, Antonio Napoli, Jaroslaw E. Prilepsky, and Sergei K. Turitsyn. Computational complexity evaluation of neural network applications in signal processing, 2022.
- [57] Chaim Baskin, Natan Liss, Eli Schwartz, Evgenii Zheltonozhskii, Raja Giryes, Alex M Bronstein, and Avi Mendelson. Uniq: Uniform noise injection for non-uniform quantization of neural networks. *ACM Transactions on Computer Systems (TOCS)*, 37(1-4):1–15, 2021.
- [58] Yann LeCun, Léon Bottou, Yoshua Bengio, and P. Haffner. Gradient-based learning applied to document recognition. *Proceedings of the IEEE*, 86(11):2278–2324, 1998.
- [59] Alex Krizhevsky, Geoffrey Hinton, et al. Learning multiple layers of features from tiny images. 2009.
- [60] Shaohui Lin, Rongrong Ji, Chenqian Yan, Baochang Zhang, Liujuan Cao, Qixiang Ye, Feiyue Huang, and David Doermann. Towards optimal structured cnn pruning via generative adversarial learning, 2019.
- [61] Xiaohan Ding, Guiguang Ding, Jungong Han, and Sheng Tang. Auto-balanced filter pruning for efficient convolutional neural networks. *Proceedings of the AAAI Conference on Artificial Intelligence*, 32(1), 2018.
- [62] Pravendra Singh, Vinay Kumar Verma, Piyush Rai, and Vinay P. Namboodiri. Leveraging filter correlations for deep model compression, 2020.
- [63] S. H. Shabbeer Basha, Mohammad Farazuddin, Viswanath Pulabaigari, Shiv Ram Dubey, and Snehasis Mukherjee. Deep model compression based on the training history, 2022.
- [64] Stefan Uhlich, Lukas Mauch, Fabien Cardinaux, Kazuki Yoshiyama, Javier Alonso Garcia, Stephen Tiedemann, Thomas Kemp, and Akira Nakamura. Mixed precision dnns: All you need is a good parametrization. *arXiv preprint arXiv:1905.11452*, 2019.
- [65] Jia Deng, Wei Dong, Richard Socher, Li-Jia Li, Kai Li, and Li Fei-Fei. Imagenet: A large-scale hierarchical image database. In *2009 IEEE conference on computer vision and pattern recognition*, pages 248–255. Ieee, 2009.
- [66] Xuanyi Dong, Junshi Huang, Yi Yang, and Shuicheng Yan. More is less: A more complicated network with less inference complexity, 2017.
- [67] Guangzhe Liu, Ke Zhang, and Meibo Lv. Soks: Automatic searching of the optimal kernel shapes for stripe-wise network pruning. *IEEE Transactions on Neural Networks and Learning Systems*, pages 1–13, 2022.
- [68] Guangzhe Liu, Ke Zhang, and Meibo Lv. Asks: Convolution with any-shape kernels for efficient neural networks. *Neurocomputing*, 446:32–49, 2021.
- [69] Xiu Su, Shan You, Fei Wang, Chen Qian, Changshui Zhang, and Chang Xu. Bcnet: Searching for network width with bilaterally coupled network, 2021.
- [70] Lucas Liebenwein, Cenk Baykal, Harry Lang, Dan Feldman, and Daniela Rus. Provable filter pruning for efficient neural networks, 2020.
- [71] Haopu Shang, Jia-Liang Wu, Wenjing Hong, and Chao Qian. Neural network pruning by cooperative coevolution, 2022.
- [72] Bin Dai, Chen Zhu, and David Wipf. Compressing neural networks using the variational information bottleneck, 2018.
- [73] Adam Paszke, Sam Gross, Francisco Massa, Adam Lerer, James Bradbury, Gregory Chanan, Trevor Killeen, Zeming Lin, Natalia Gimelshein, Luca Antiga, Alban Desmaison, Andreas Köpf, Edward Yang, Zach DeVito, Martin Raison, Alykhan Tejani, Sasank Chilamkurthy, Benoit Steiner, Lu Fang, Junjie Bai, and Soumith Chintala. Pytorch: An imperative style, high-performance deep learning library, 2019.

- [74] Zhuohan Li, Eric Wallace, Sheng Shen, Kevin Lin, Kurt Keutzer, Dan Klein, and Joey Gonzalez. Train big, then compress: Rethinking model size for efficient training and inference of transformers. In *International Conference on Machine Learning*, pages 5958–5968. PMLR, 2020.
- [75] Jacob Devlin, Ming-Wei Chang, Kenton Lee, and Kristina Toutanova. Bert: Pre-training of deep bidirectional transformers for language understanding. *arXiv preprint arXiv:1810.04805*, 2018.
- [76] Richard Socher, Alex Perelygin, Jean Wu, Jason Chuang, Christopher D. Manning, Andrew Ng, and Christopher Potts. Recursive deep models for semantic compositionality over a sentiment treebank. In *Proceedings of the 2013 Conference on Empirical Methods in Natural Language Processing*, pages 1631–1642, Seattle, Washington, USA, October 2013. Association for Computational Linguistics.
- [77] Adina Williams, Nikita Nangia, and Samuel R. Bowman. A broad-coverage challenge corpus for sentence understanding through inference, 2018.
- [78] Alex Wang, Amanpreet Singh, Julian Michael, Felix Hill, Omer Levy, and Samuel R Bowman. Glue: A multi-task benchmark and analysis platform for natural language understanding. *arXiv preprint arXiv:1804.07461*, 2018.
- [79] Pranav Rajpurkar, Jian Zhang, Konstantin Lopyrev, and Percy Liang. Squad: 100,000+ questions for machine comprehension of text, 2016.
- [80] Woosuk Kwon, Sehoon Kim, Michael W. Mahoney, Joseph Hassoun, Kurt Keutzer, and Amir Gholami. A fast post-training pruning framework for transformers, 2022.
- [81] Neo Wei Ming, Zhehui Wang, Cheng Liu, Rick Siow Mong Goh, and Tao Luo. Ma-bert: Towards matrix arithmetic-only bert inference by eliminating complex non-linear functions. In *The Eleventh International Conference on Learning Representations*, 2023.
- [82] Tsung-Yi Lin, Michael Maire, Serge Belongie, Lubomir Bourdev, Ross Girshick, James Hays, Pietro Perona, Deva Ramanan, C. Lawrence Zitnick, and Piotr Dollár. Microsoft coco: Common objects in context, 2015.
- [83] Michela Paganini. Prune responsibly, 2020.
- [84] Steven K. Esser, Jeffrey L. McKinstry, Deepika Bablani, Rathinakumar Appuswamy, and Dharmendra S. Modha. Learned step size quantization, 2020.
- [85] Jungwook Choi, Zhuo Wang, Swagath Venkataramani, Pierce I-Jen Chuang, Vijayalakshmi Srinivasan, and Kailash Gopalakrishnan. Pact: Parameterized clipping activation for quantized neural networks. *arXiv preprint arXiv:1805.06085*, 2018.
- [86] Erich Elsen, Marat Dukhan, Trevor Gale, and Karen Simonyan. Fast sparse convnets, 2019.
- [87] Trevor Gale, Matei Zaharia, Cliff Young, and Erich Elsen. Sparse gpu kernels for deep learning, 2020.
- [88] Yaohui Cai, Weizhe Hua, Hongzheng Chen, G. Edward Suh, Christopher De Sa, and Zhiru Zhang. Structured pruning is all you need for pruning cnns at initialization, 2022.

A Further Algorithmic Details

A.1 Standard Information Geometric Results

Proposition A.1. *The FIM defines an estimate for the natural metric tensor of the statistical manifold induced by the parameterized model, obtained infinitesimally from an expansion of the KL divergence.*

Proof. Here we describe the discrete case; however, the continuous follows similarly.

$$\begin{aligned}
D_{KL}(p_\theta || p_{\theta+\delta\theta}) &= \sum_D p_\theta \log \frac{p_\theta}{p_{\theta+\delta\theta}} \\
&\approx \sum_D p_\theta \log p_\theta - p_\theta \left[\log p_\theta + \frac{\nabla_\theta p_\theta^T}{p_\theta} \delta\theta + \frac{1}{2} \delta\theta^T \left(\frac{\nabla_\theta^2 p_\theta}{p_\theta} - \frac{\nabla_\theta p_\theta \nabla_\theta p_\theta^T}{p_\theta^2} \right) \delta\theta \right] \\
&\approx - \left[\sum_D \nabla_\theta p_\theta \right]^T \delta\theta - \frac{1}{2} \delta\theta^T \left[\sum_D \nabla_\theta^2 p_\theta \right] \delta\theta + \frac{1}{2} \delta\theta^T \left[\sum_D p_\theta \nabla_\theta \log p_\theta \nabla_\theta \log p_\theta^T \right] \delta\theta \\
&\approx - \left[\nabla_\theta \sum_D p_\theta \right]^T \delta\theta - \frac{1}{2} \delta\theta^T \left[\nabla_\theta^2 \sum_D p_\theta \right] \delta\theta + \frac{1}{2} \delta\theta^T \left[\sum_D p_\theta \nabla_\theta \log p_\theta \nabla_\theta \log p_\theta^T \right] \delta\theta \\
&\approx \frac{1}{2} \delta\theta^T \left[\sum_D p_\theta \nabla_\theta \log p_\theta \nabla_\theta \log p_\theta^T \right] \delta\theta \\
&\approx \frac{1}{2} \delta\theta^T \left[\frac{1}{N} \sum_D \nabla_\theta \log p_\theta \nabla_\theta \log p_\theta^T \right] \delta\theta \\
&= \frac{1}{2} \delta\theta^T \hat{I}(\theta) \delta\theta
\end{aligned}$$

□

In Riemannian geometry, Rao's distance measure between two points on the statistical manifold (θ_1, θ_2) follows from the integral of these quadratic differentials along a path joining θ_1 and θ_2 , given by:

$$\left| \int_{\theta_1}^{\theta_2} [\delta\theta^T I(\theta) \delta\theta]^{\frac{1}{2}} \right| \quad (7)$$

The geodesic (shortest path) between these two points is typically of interest.

A.2 The FIT Approximation

Recent work stochastically approximates the EF [43].

Proposition A.2. *FIT is obtained (under mild noise assumptions) by taking an expectation over the Fisher-Rao quadratic differential.*

Proof.

$$\begin{aligned}
\Omega &= \mathbb{E} [\delta\theta^T I(\theta) \delta\theta] \\
&= \mathbb{E}[\delta\theta]^T I(\theta) \mathbb{E}[\delta\theta] + \text{Tr}(I(\theta) \text{Cov}[\delta\theta])
\end{aligned}$$

It is assumed that the random compression noise is symmetrically distributed around a mean of zero: $\mathbb{E}[\delta\theta] = 0$, and uncorrelated: $\text{Cov}[\delta\theta] = \text{Diag}(\mathbb{E}[\delta\theta^2])$. This yields the FIT heuristic:

$$\Omega = \text{Tr} (I(\theta) \text{Diag}(\mathbb{E}[\delta\theta^2]))$$

This is employed in an approximate form:

$$\Omega = \sum_l^L Tr(\hat{I}(\theta_l)) \cdot Diag(\hat{\mathbb{E}}_l[\delta\theta^2]).$$

□

In this case, the trace of the EF admits a very simple computational form:

Proposition A.3. *The trace of the EF can be computed via the sum of the square of the gradient.*

Proof. The trace is a linear operator, which allows each individual estimator to be extracted from the summation. Additionally, the trace of the second moment matrix can then be computed by the norm of the vector of parameters from which it is composed:

$$\begin{aligned} Tr[\hat{I}(\theta)] &= Tr \left[\frac{1}{N} \sum_{i=1}^N \nabla f(z_i, \theta) \nabla f(z_i, \theta)^T \right] \\ &= \frac{1}{N} \sum_{i=1}^N Tr [\nabla f(z_i, \theta) \nabla f(z_i, \theta)^T] \\ &= \frac{1}{N} \sum_{i=1}^N \nabla f(z_i, \theta)^T \nabla f(z_i, \theta) \\ &= \frac{1}{N} \sum_{i=1}^N \|\nabla f(z_i, \theta)\|^2 \end{aligned}$$

□

B Ablation Study

In this section, we perform an ablation study to highlight the importance of path planning in FIT-Compress. In particular, we compare FITCompress with the quantize-then-prune ($Q_{FIT} + P_{FIT}$) and prune-then-quantize ($P_{FIT} + Q_{FIT}$) regimes. For Q_{FIT} , we generate several quantization configurations using the FIT sensitivity metric. This is then combined with P_{FIT} , where we prune with FIT as an importance heuristic using manually-selected pruning percentages to fulfill the desired compression constraint. Our ablation study repeats the findings of [51] (i.e. pruning and quantization are non-commutative). Results are displayed in Figure 6.

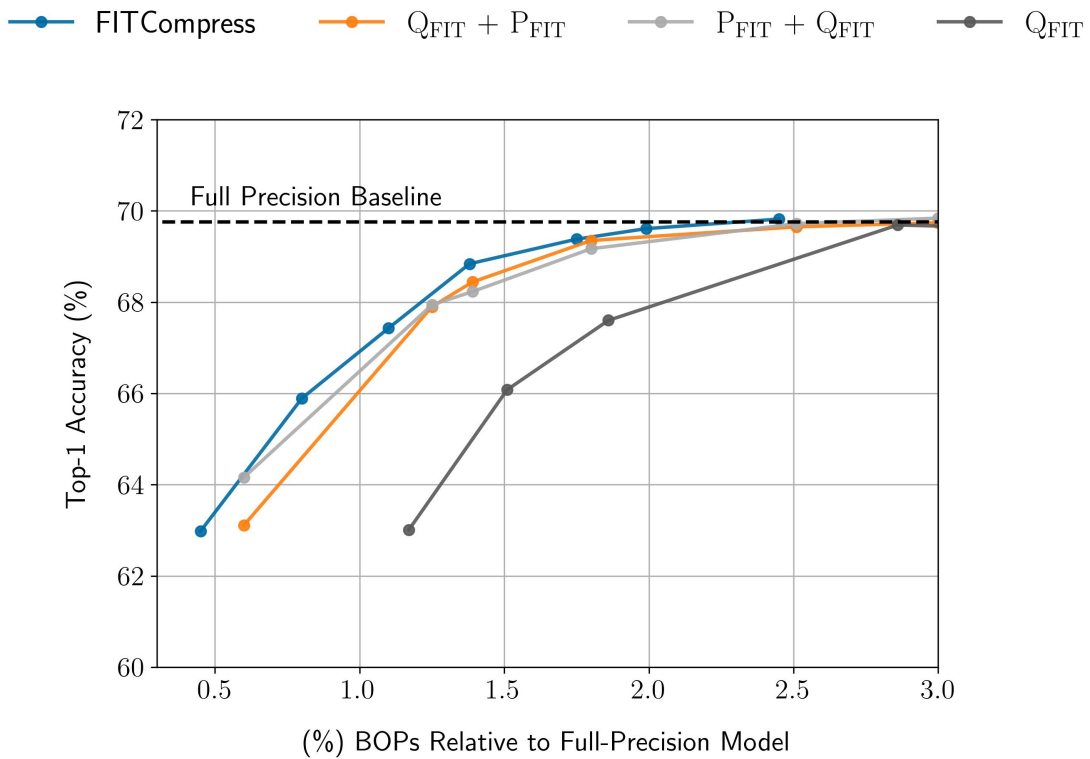


Figure 6: Comparing FITCompress with sequential applications of quantization and pruning at different compression levels. For reference we also include quantization only. We do not include pruning only. This is because we cannot simultaneously compress ResNet-18 to the 0.5-3% relative BOPs range with pruning only and preserve top-1 accuracy above 60% on ImageNet.

C Experimental Setup

In this section, we detail our full experimental set-up. Additional optimization can be made in the training recipe, but this lies outside the scope of our study. We use NVIDIA A100-SXM4 40GB GPUs. We estimate that our total usage emits approximately 30 kgCO₂eq.

Table 4: We list the hyperparameters that we used to find the optimal configuration and to train the models presented in Tables 1, 2 and 3, as well as Figure 5.

	LeNet-5 on MNIST	VGG-7 on CIFAR-10	ResNet-18/34/50 on ImageNet	BERT-Base on NLP Tasks	YOLOv5m on COCO
Optimizer	Adam	Adam	SGD	AdamW	SGD
Scheduler	Cosine Annealing LR	Cosine Annealing LR	Cosine Annealing LR	Linear	Lambda LR
Epochs	120	300	90	(3, 5)	300
Batch Size	128	128	128	32	256
Learning Rate	10^{-3}	10^{-3}	5×10^{-3}	$(2, 5) \times 10^{-5}$	10^{-2}
Weight Decay	0	0	5×10^{-4}	0	5×10^{-5}
Quantization schedule Q	2, 3, 4, 5	2, 3, 4, 5, 8	2, 3, 4, 5, 8	2, 3, 4, 5, 8	4, 8, 10, 12, 14, 16
Pruning schedule κ	$1 - 10^{-\frac{n}{40}}, n = 1, \dots, 40$	$1 - 10^{-\frac{n}{40}}, n = 1, \dots, 40$	$1 - 10^{-\frac{n}{40}}, n = 1, \dots, 40$	$1 - 10^{-\frac{n}{40}}, n = 1, \dots, 40$	$1 - 10^{-\frac{n}{40}}, n = 1, \dots, 40$

D FITCompress Model Configurations

In this section, we provide detailed visualizations of the pruning and MPQ configurations obtained via FITCompress for each model discussed in Section 4.

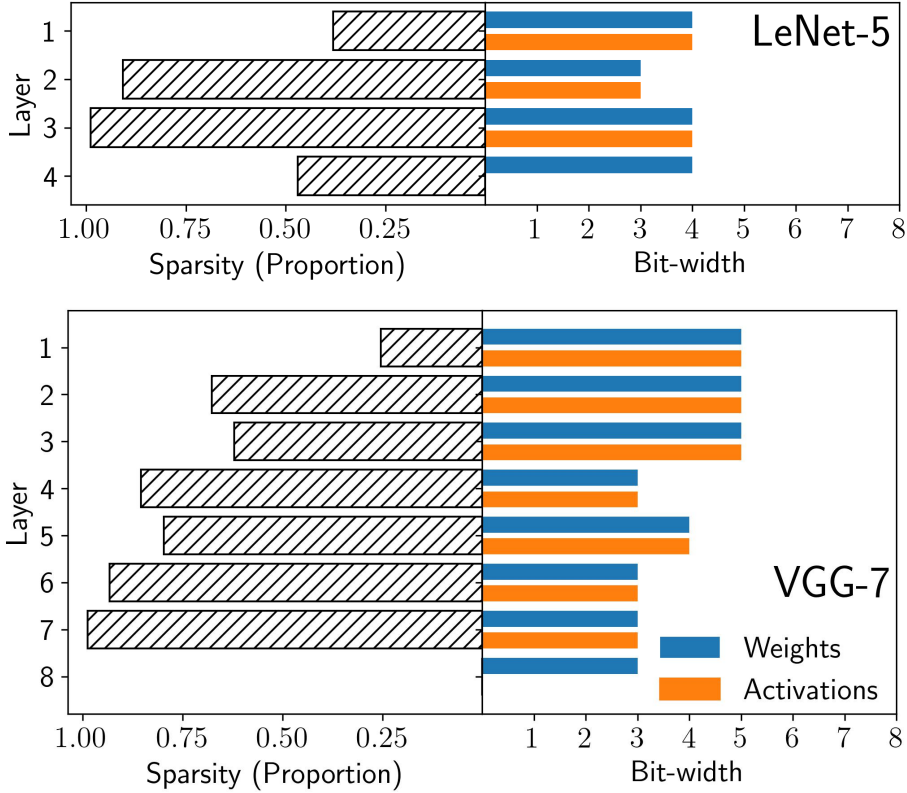


Figure 7: FITCompress-generated model configurations for LeNet-5 and VGG-7.

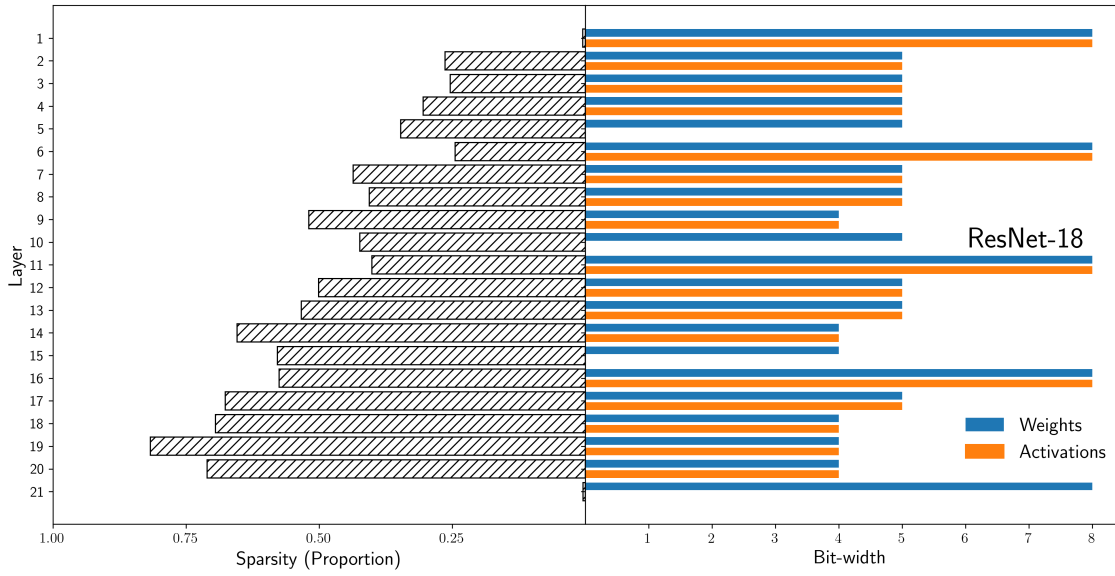


Figure 8: FITCompress-generated model configuration for ResNet-18.

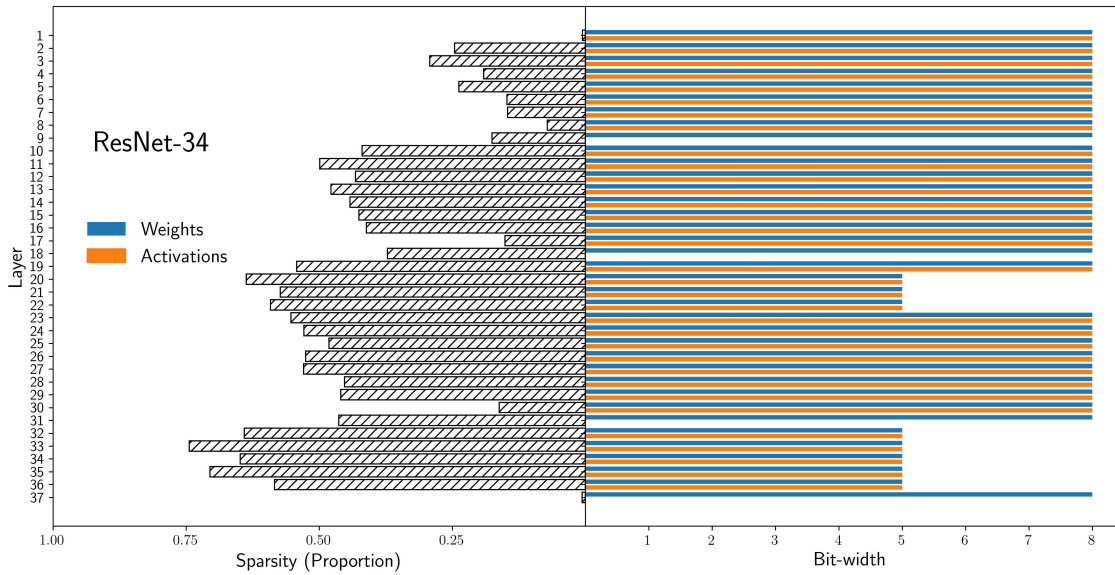


Figure 9: FITCompress-generated model configuration for ResNet-34.

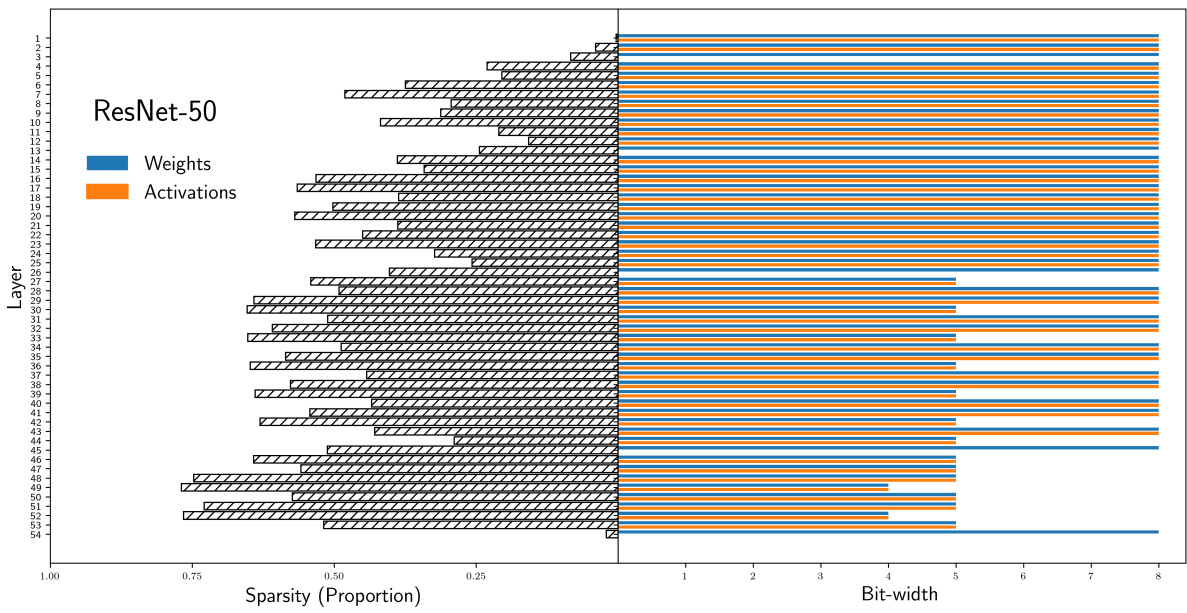


Figure 10: FITCompress-generated model configuration for ResNet-50.

E A Comment on Unstructured Pruning

In contrast to methods that combine MPQ with structured pruning (e.g. BB and DJPQ), FITCompress combines MPQ with unstructured pruning. This has the advantage of yielding models with more sparsity and higher weight and activation precision compared to methods like BB and DJPQ (see Section 4). While structured pruning is typically favored over unstructured pruning in literature, several authors provide promising methods that are bridging the gap [86, 87]. Secondly, unstructured pruning has been shown to yield higher performing models compared to structured pruning methods [88, 17]. We also tested unstructured sparsity on hardware to challenge the idea that it may be hardware-unfriendly. Our experiments suggest that unstructured pruning can drastically accelerate neural network operations like convolution compared to the unpruned case. We illustrate this in Figure 11.

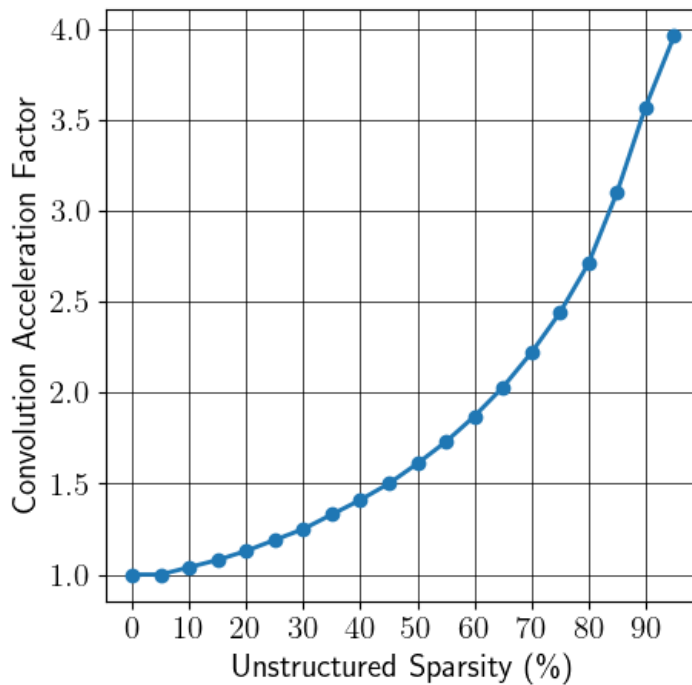


Figure 11: Acceleration of convolution vs. unstructured sparsity measured directly on a NeuPro-M processing chip. The pruning acceleration was calculated on synthesized data where zeroes were randomly distributed across weight vectors in ResNet-50.